

ENHANCED RAINFALL IN THE WESTERN MEDITERRANEAN DURING DEPOSITION OF SAPROPEL S1: STALAGMITE EVIDENCE FROM CORCHIA CAVE (CENTRAL ITALY)

Zanchetta G.¹, Drysdale R.N.², Hellstrom J.C.³, Fallick A.E.⁴, Isola I.⁵, Gagan, M.⁶, Pareschi M.T.⁵

¹Dipartimento di Scienze della Terra, University of Pisa, Via S. Maria 53, 56126 Pisa Italy

²School of Environmental and Life Sciences, University of Newcastle, Callaghan, NSW 2308, Australia

³School of Earth Sciences, University of Melbourne, Parkville, Victoria 3010 Australia

⁴Scottish Universities Environmental Research Centre, East Kilbride, G75 0GF Glasgow, UK

⁵Istituto Nazionale di Geofisica e Vulcanologia, Sezione di Pisa, Via della Faggiola 32, 56126 Pisa, Italy

⁶Research School of Earth Sciences, The Australian National University, Canberra ACT 0600, Australia

Abstract

A stable isotope record from a stalagmite collected from Antro del Corchia cave (Apuan Alps, Central Italy), supported by 17 uranium-series ages, indicates enhanced regional rainfall between ca. 8.9 and 7.3 kyr cal. BP at the time of sapropel S1 deposition. Within this phase, the highest rainfall occurred between 7.9 and 7.4 kyr cal. BP. Comparison with different marine and lake records, and in particular with the Soreq Cave record (Israel), suggests substantial in-phase occurrence of enhanced rainfall between the Western and Eastern Mediterranean basins. There is no convincing evidence for major climatic change at the time of the “8.2 ka event”.

Keywords: speleothems, Corchia Cave, sapropel S1, stable isotopes, Italy

1. Introduction

In contrast to the last glacial period, climate proxy records show that the Holocene has been characterised by only minor temperature fluctuations (Alley et al., 1997). However, significant oceanographic and hydrologic changes have occurred, particularly in the middle and low latitudes (Mayewski et al., 2004). A notable example is the climate associated with sapropel S1, which was deposited in the eastern and central Mediterranean basins during the Early-Mid Holocene (ca. 6600-9500 yr cal BP: e.g. Emeis et al., 2000). Sapropels are organic-carbon-rich layers usually found intercalated with the more typical organic-poor carbonate sediments of the Mediterranean. Several hypotheses exist on the origin of sapropels (e.g. Rohling, 1994; Emeis et al., 2000). Many of these invoke an increase in terrestrial runoff, most likely from the Nile basin (Krom et al. 2002; Sperling et al. 2003). This runoff appears to have reduced surface-water salinity, with consequent deep-water stratification and anoxia (Emeis et al. 2000). Sapropels are climatically significant because they are thought to be linked to episodes of enhanced monsoon activity corresponding to minima in Earth's orbital precession (Rossignol-Strick et al., 1982; Emeis et al. 2000).

Most of the lithostratigraphic evidence for S1 is found in marine cores of the Adriatic Sea, and the Ionian and Levantine Basins (Emeis et al., 2000; Giunta et al., 2003; Fig. 1). However, its distribution through these basins is discontinuous (Ariztegui et al., 2000), and its timing is difficult to constrain due to varying degrees of preservation, problems with calibrating marine radiocarbon ages and the spatial complexity of the circulation and biogeochemical changes which took place (e.g. Thomson et al., 1999; Siani et al., 2001). In spite of its tropical origin, there is increasing evidence that the zone which experienced increased rainfall at this time included the Mediterranean region itself (Rossignol-Strick, 1999; Kallel et al., 1997, 2000; Bar-Matthews et al., 2000, 2003; Magny et al., 2002). In order to better define the climatic conditions throughout the Mediterranean region and to assist in land-sea correlations of this event, well-dated terrestrial records are needed from archives sensitive to millennial-scale changes in regional hydrology.

Speleothems are cave calcium carbonate deposits with a demonstrated capacity for preserving climate changes during Mediterranean sapropel events (Bar-Matthews et al., 2000;2003; Bard et al., 2002). In this paper, we present a precisely dated isotopic record from a speleothem collected from Antro del Corchia, central Italy, which displays direct evidence of increased rainfall in the region during the period of S1 deposition and provides an opportunity for correlation with nearby marine- and lake-core records.

2. Methods

Our data are derived from a ca. 25 cm-tall inactive stalagmite (CC26) collected *in situ* from a deep chamber within Antro del Corchia (43° 59' N, 10° 13' E; Fig. 1). The regional setting and cave characteristics are described in detail by Drysdale et al. (2004). After sectioning, the internal stratigraphy of CC26 revealed several phases of deposition (Fig. 1). Radiometric ^{230}Th - ^{234}U dating of 17 samples by multi-collector inductively coupled plasma mass spectrometry (Hellstrom, 2003; Table 1) revealed that the upper ca. 160 mm section grew continuously from the Late Glacial to the Little Ice Age. This upper section was microsampled for stable isotope analysis at a 200 μm interval. The powders were processed using an Analytical Precision AP2003 continuous-flow stable isotope ratio mass spectrometer. The stable isotope data were fitted to a depth-age model using a technique previously described by Drysdale et al. (2005) (Fig. 2). All ages are reported as calendar years. Further details of analytical methods are provided in the Supplementary Material.

3. Results and interpretation

The complete isotope time series is shown in Figure S1 of the Supplementary Material. Here we focus on the interval from 5 to 10 kyr, which brackets the period of S1 deposition. The most prominent feature of this interval in the CC26 record is the reduction in $\delta^{18}\text{O}$ that commences

stepwise at ca. 8.9 kyr and terminates abruptly at 7.3 kyr (Fig. 2). Three possible mechanisms may explain this interval of low $\delta^{18}\text{O}$ values. The first concerns changes in regional air temperatures, which can alter air temperatures inside the cave (Gascoyne, 1992). Cave air temperature controls the degree of isotopic fractionation between cave drip waters and the calcite deposited from them. If drip water $\delta^{18}\text{O}$ remains constant, an increase in cave temperature will cause a reduction in calcite $\delta^{18}\text{O}$ at a rate of ca. $-0.24\text{‰}/^{\circ}\text{C}$ (at temperatures between 5 and 10°C : Kim and O'Neill, 1997). However, previous speleothem work from western Italy has shown that cave-temperature effects are likely to be counterbalanced by the influence of changing regional air temperatures on rainfall $\delta^{18}\text{O}$, which is estimated to be $0.2\text{-}0.3\text{‰}/^{\circ}\text{C}$ (Bard et al., 2002). Hence, if a temperature increase alone occurred, it would have had an indistinguishable effect on speleothem $\delta^{18}\text{O}$ at this site.

A second possible mechanism is the “rainfall amount” effect (Dansgaard, 1964), where rainfall $\delta^{18}\text{O}$ decreases as rainfall amount increases. This is regarded as a principal mechanism driving variations in rainfall $\delta^{18}\text{O}$ (and therefore drip-water and speleothem $\delta^{18}\text{O}$ values) in the Mediterranean region (Bar-Matthews et al., 2000; Bard et al., 2002). In previously studied Corchia stalagmites, intervals of low $\delta^{18}\text{O}$ correspond to wetter and warmer climatic periods (Drysdale et al., 2004; 2005), suggesting that the amount effect is coupled to regional temperatures. Such a coupling presumably arises due to greater evaporation from warmer versus cooler sea surfaces in the moisture source regions (i.e. the North Atlantic and Western Mediterranean).

A third possibility is a change in the composition of the vapour source. Studies of Western Mediterranean marine cores show evidence of reduced sea-surface $\delta^{18}\text{O}$ during the time of S1 formation (e.g. Emeis et al., 2000; Kallel et al., 1997; 2000). For example, compared to the beginning of the Holocene, evidence from the Alboran and Southern Tyrrhenian Seas suggests a salinity decrease of ca. 3‰ during S1 deposition (Kallel et al., 1997; 2000; Emeis et al., 2000). This

decrease was partially recovered at the end of sapropel deposition. Today, the $\delta^{18}\text{O}$ /salinity ratio for the Mediterranean Sea is ca. 0.26 (Pierre, 1999). Although this ratio may have been higher during S1 deposition (e.g. Emeis et al., 2000), a first-order estimate of the reduction in sea-surface $\delta^{18}\text{O}$ during S1 based on the above ratio is ca. 0.8 ‰. This may have been partly attributed to increased runoff to the marine environment from higher rainfall over continental areas bordering the Mediterranean (e.g. Kallel et al., 1997). Given that the Western Mediterranean supplies about 40% of the moisture reaching central-western Italy (Bard et al., 2002), a more ^{18}O -depleted sea surface would have caused a reduction in the $\delta^{18}\text{O}$ of vapour, leading to a depletion in the isotopic composition of the recharge waters reaching the cave.

Whilst there is marine-core evidence for a change in moisture-source composition, support for rainfall amount must be sought from other properties of CC26. One potential source of supporting data is the $\delta^{13}\text{C}$ time series. The full Holocene $\delta^{13}\text{C}$ time series for CC26 displays the typical interglacial pattern found in older Corchia speleothems, where isotopic values steadily decrease the further an interglacial progresses (Figure S1), probably due to the time lag required for post-glacial soils to establish above the cave (Drysedale et al., 2004). The range of $\delta^{13}\text{C}$ values in CC26 is comparable with those predicted from the $\delta^{13}\text{C}$ of the dissolved inorganic carbon in modern cave drip waters ($-4.1 \pm 0.6\text{‰}$; Doveri et al., 2005). Such an enrichment in ^{13}C can be attributed to the relatively high $\delta^{13}\text{C}$ of the source rock (up to $+2.5\text{‰}$) and to the low contribution from soil CO_2 . The latter would be expected from a recharge area characterised by steep terrain, very low soil cover and sparse vegetation. Since the rock value is time-constant, periodic change in soil CO_2 production is the most likely factor driving $\delta^{13}\text{C}$ variations.

Removing the long-term trend in $\delta^{13}\text{C}$ reveals its shorter-term structure (Figure S1). Between 5 and 10 kyr, the $\delta^{13}\text{C}$ displays a complex pattern of multi-centennial-scale oscillations. However, several

of these oscillations are superimposed over a relatively broad and prominent interval of decreased $\delta^{13}\text{C}$ extending between ca. 8.5 and 7.3 kyr, with the most ^{13}C -depleted values found between ca. 7.9 and 7.4 kyr (Fig. 2). Increases in rainfall and temperature can increase soil CO_2 productivity (e.g. Raich and Schlesinger, 1992) and reduce speleothem $\delta^{13}\text{C}$ (Genty et al., 2003). Increased rainfall can also limit the opportunity of prior calcite precipitation during seepage (Fairchild et al., 2000), a process that may enrich $\delta^{13}\text{C}$ along the percolation pathway due to excessive degassing of CO_2 . Thus, the broad period of lower values between ca. 8.5 and 7.3 kyr probably reflects an increased input of soil CO_2 , potentially due to increased rainfall and temperatures, and/or a rainfall-driven decrease in prior calcite precipitation along the flow path. The period of lowest $\delta^{13}\text{C}$ values substantially matches the plateau of lowest $\delta^{18}\text{O}$ values, which possibly indicates the period of maximum amount of rainfall through S1 in this part of the Mediterranean (ca. 7.9 to 7.4 kyr).

Therefore, the coupled $\delta^{18}\text{O}$ and $\delta^{13}\text{C}$ evidence from CC26 suggests an increase in rainfall at the site. This increase in rainfall appears to have reduced sea-surface salinity in the Western Mediterranean Sea, and in turn the isotopic composition of the derived vapour.

4. Discussion and conclusions

The timing of the shift in $\delta^{18}\text{O}$ (8.9 ± 0.2 to 7.3 ± 0.2 kyr) is consistent with recent estimates of the duration of S1 inferred from marine cores taken adjacent to the Italian peninsula (Ariztegui et al., 2000; Giunta et al., 2003; Rolph et al., 2004). The central Italian crater lakes of Albano and Nemi (Fig. 1) also preserve evidence for warmer and wetter conditions during S1 deposition (Ariztegui et al., 2000; Rolph et al., 2004), although establishing the precise timing of the inferred S1 interval from these sites is difficult due to dating uncertainties (Oldfield, 1996). The timing is also broadly consistent with the speleothem record from Soreq Cave (Israel), where the event is bracketed between 8.5 and 7 kyr (Fig. 3; Bar-Matthews et al. 2000). The small age offset between the two

records has to be considered in the context of age uncertainties. During this interval, the Soreq $\delta^{18}\text{O}$ attains its lowest Holocene values, consistent with the rainfall amount effect which has been invoked as a major driver of $\delta^{18}\text{O}$ over the last 240 kyr at this site (Bar-Matthews et al., 2000; 2003), whereas the $\delta^{13}\text{C}$ shows an extreme increase of up to $\sim 8\text{‰}$ during S1, presumably due to a reduction in biogenic CO_2 input to the percolation waters caused by either catastrophic soil erosion or a percolation rate so rapid that CO_2 equilibration between infiltration water and soil air was not attained (Bar-Matthews et al., 2000).

Many eastern and central Mediterranean marine sites preserve an interruption in S1 deposition, which is usually manifested as a break in organic-rich mud deposition, thought to reflect a brief return to deep-water ventilation (Rohling et al., 1997; De Rijk et al., 1999; Ariztegui et al., 2000; Giunta et al., 2003). The duration and the precise timing of this interruption is debated (e.g. Rohling et al., 1997; Ariztegui et al., 2000; Giunta et al., 2003), with estimates varying from ca. 500 to 150 yr during the interval ca 8.0-7.5 kyr (Ariztegui et al., 2000). It is equivocal whether such an interruption is preserved in CC26. Closer inspection reveals at least two minor “reversals” in isotopic trends (e.g. at ca 8.3 and 8.6 kyr; Fig. 2), but these are of relatively low magnitude. This precludes a direct correlation of the S1 interruption with the CC26 record.

In many records of the Northern Hemisphere there is a prominent climatic deterioration centred at 8.2 kyr (Alley et al., 1997; Alley and Ágústsdóttir, 2005). The lack of prominence of such an event in CC26 is surprising given its apparent widespread extent. Pollen records from Lago di Vico (Magri and Parra, 2002) suggest that in central Italy at ca. 8.1 kyr there is a prominent decrease in arboreal cover indicating drier conditions, which might be consistent with the minor $\delta^{18}\text{O}$ reversal observed in the CC26 record at ca 8.3 kyr. However, Emeis et al. (2000) did not find evidence for an increase of surface salinity in the Western Mediterranean Sea at this time, as would be expected from reduced continental runoff, whilst in the eastern part of the basin an increase of surface sea

salinity is evident (Emeis et al., 2000). This indicates that the Western Mediterranean surface water was still depleted in ^{18}O , which may have buffered the isotopic signal in the rainfall reaching the cave.

In conclusion, the stable isotope record from CC26 provides the first precisely dated evidence for enhanced rainfall in the Western Mediterranean basin during the time of sapropel S1 formation. The combined $\delta^{18}\text{O}$ and $\delta^{13}\text{C}$ evidence suggests the phase of highest rainfall probably occurred between 7.9 and 7.4 kyr, whilst comparison with different marine and lake records, and, in particular, with the Soreq Cave record, indicates substantial in-phase occurrence of enhanced rainfall between Western and Eastern Mediterranean basins.

5. Acknowledgements

The authors are indebted to Federazione Speleologica Toscana for the funding of this research, and A. Tait and T. Donnelly for the analytical support for the stable isotope measurements. SUERC is funded by a consortium of Scottish Universities and NERC. RD acknowledges the financial support of the Research Management Committee of the University of Newcastle.

6. References

Alley, R.B., Mayewsky, P.A., Sowers, T., Stuiver, M., Taylor, K.C., Clark, P.U., 1997. Holocene climatic instability: a prominent, widespread event 8200 yr ago. *Geology* 25, 483-486.

Alley, R.B., Ágústsdóttir, A.M., 2005. The 8k event: cause and consequences of a major Holocene abrupt climate changes. *Quaternary Science Reviews* 24, 1123-1149.

Ariztegui, D., Asioli, A., Lowe, J.J., Trincardi, F., Vigliotti, L., Tamburini, F., Chondrogianni, C., Accorsi, C.A., Bandini Mazzanti, M., Mercuri, A.M., Van der Kaars, S., McKenzie, J.A., Oldfield, F., 2000. Palaeoclimate and the formation of sapropel S1: inferences from Late Quaternary lacustrine and marine sequences in the central Mediterranean region. *Palaeogeography, Palaeoclimatology, Palaeoecology* 158, 215-240.

Bard, E., Delaygue, G., Rostek, F., Antonioli, F., Silenzi, S., Schrag, D., 2002. Hydrological conditions in the western Mediterranean basin during the deposition of Sapropel 6 (ca. 175 kyr). *Earth and Planetary Science Letters* 202, 481-494.

Bar-Matthews, M., Ayalon, A., Kaufmann, A., 2000. Timing and hydrological conditions of sapropel events in the eastern Mediterranean, as evident from speleothems, Soreq Cave, Israel. *Chemical Geology* 169, 145-156.

Bar-Matthews, M., Ayalon, A., Gilmour, M., Matthews, A., Hawkesworth, C.J., 2003. Sea-land oxygen isotopic relationship from planktonic foraminifera and speleothems in the Eastern Mediterranean region and their implication for paleorainfall during interglacial intervals. *Geochimica et Cosmochimica Acta* 67, 3181-3199.

Dansgaard, W., 1964, Stable isotopes in precipitation: *Tellus* 4, 436-468.

De Rijk, S., Hayes, A., Rohling, E.J., 1999. Eastern Mediterranean sapropel S1 interruption: an expression of the onset of climatic deterioration around 7 ka BP. *Marine Geology* 153, 337-343.

Doveri, M., Leone, G., Mussi, M., Zanchetta, G., 2005. Composizione isotopica di acque ipogee dell'Antro del Corchia (Alpi Apuane, Toscana Nord-Occidentale). *Memorie Istituto Italiano Speleologia* s. 2, 18, 119-132.

Drysdale, R.N., Zanchetta, G., Hellstrom, J.C., Fallick, A.E., Zhao, J-x., Isola, I., Bruschi, G., 2004. Palaeoclimatic implications of the growth history and stable isotope ($\delta^{18}\text{O}$ and $\delta^{13}\text{C}$) geochemistry of a Middle to Late Pleistocene stalagmite from central-western Italy. *Earth and Planetary Science Letters* 227, 215-229.

Drysdale, R.N., Zanchetta, G., Hellstrom, J.C., Fallick, A.E., Zaho J.-x., 2005. Stalagmite evidence for the onset of the Last Interglacial in southern Europe at 129 ± 1 ka. *Geophysical Research Letters*, 32, L24708, doi:10.1029/2005GL024658.

Emeis, K-C., Struck, U., Schulz, H-M., Rosenberg, R., Bernasconi, S., Erlekeuser, H., Sakamoto, T., Martinez-Ruiz, F., 2000. Temperature and salinity variations of Mediterranean Sea surface waters over the last 16,000 years from records of planktonic stable oxygen isotopes and alkenone unsaturation ratios. *Palaeogeography, Palaeoclimatology, Palaeoecology* 158, 259-280.

Fairchild, I.J., Borsato, A., Tooth, A.F., Frisia, S., Hawkesworth, C.J., Huang, Y., McDermott, F., Spiro, B., 2000. Controls on trace element (Sr-Mg) composition of carbonate cave waters: implications for speleothem climatic records. *Chemical Geology* 166, 255-269.

Gascoyne, M., 1992. Palaeoclimate determination from cave calcite deposits. *Quaternary Science Reviews* 11, 609-632.

Genty, D., Blamart, D., Ouahdi, R., Gilmour, M., Baker, A., Jouzel, J., Van-Exter, S., 2003. Precise dating of Dansgaard-Oeschger climate oscillations in the western Europe from stalagmite data. *Nature* 421, 833-837.

Giunta, S., Negri, A., Morigi, C., Capotondi, L., Combourieu-Nebout, N., Emeis, K.C., Sangiorgi F., Vigliotti, L., 2003. Coccolithophorid ecostratigraphy and multi-proxy paleoceanographic reconstruction in the Southern Adriatic Sea during the last deglaciation time (Core AD91-17). *Palaeogeography, Palaeoclimatology, Palaeoecology* 190, 39-59.

Hellstrom, J.C., 2003. Rapid and accurate U/Th dating using parallel ion-counting multi-collector ICP-MS. *Journal of Analytical Atomic Spectrometry* 18, 135-136.

Kallel, N., Paterne, M., Labeyrie, L., Duplessy, J.-C., Arnold, M., 1997. Temperature and salinity records of the Tyrrhenian Sea during the last 18,000 years. *Palaeogeography, Palaeoclimatology, Palaeoecology* 135, 97-108.

Kallel, N., Duplessy, J.-C., Labeyrie, L., Fontugne, M., Paterne, M., Montacer, M., 2000. Mediterranean pluvial periods and sapropel formation over the last 200 000 years. *Palaeogeography, Palaeoclimatology, Palaeoecology* 157, 45-58.

Kim, S.-T., O'Neil, J.R., 1997. Equilibrium and non-equilibrium oxygen isotope effect in synthetic carbonates. *Geochimica et Cosmochimica Acta* 61, 3461-3475.

Magri, D., Parra, I., 2002. Late Quaternary western Mediterranean pollen records and African winds. *Earth and Planetary Science Letters* 200, 401-408.

Mayewski, P.A., Rohling, E.E., Stager, J.C., Karlén, W., Maasch, K.A., Meeker, L.D., Meyerson, E.A., Gasse, F., van Kreveld, S., Holmgren, K., Lee-Thorp, J., Rosqvist, G., Rack F., Staubwasser, M., Schneider, R.R., Steig, E.J., 2004. Holocene climate variability. *Quaternary Research* 62, 243-255.

Magny, M., Miramont, C., Sivan, O., 2002. Assessment of the impact of climate and anthropogenic factors on Holocene Mediterranean vegetation in Europe on the basis of palaeohydrological records. *Palaeogeography, Palaeoclimatology, Palaeoecology* 186, 47-59.

Oldfield, F., 1996. The PALICLAS Project: synthesis and overview. In: Oldfield, F., Gulizzoni, P. (Eds), *Palaeoenvironmental analysis of Italian crater Lake and Adriatic sediments. Memorie Istituto Italiano Idrobiologia* 55, 329-357.

Pierre, C., 1999. The oxygen and carbon isotope distribution in the Mediterranean water masses. *Marine Geology* 153, 41-55.

Raich, J. W., Schlesinger, W. H. 1992. The global carbon dioxide flux in soil respiration and its relationship with vegetation and climate. *Tellus* 44B, 81-99.

Rohling, E.J., 1994. Review and new aspects concerning the formation of eastern Mediterranean sapropels. *Marine Geology* 122, 1-28.

Rohling, E.J., Jorissen, F.J., De Stigter, H.C., 1997. 200 yr interruption of Holocene sapropel formation in the Adriatic Sea. *Journal of Micropalaeontology* 16, 97-108.

Rolph, T.C., Vigliotti, L., Oldfield, F., 2004. Mineral magnetism and geomagnetic secular variation of marine and lacustrine sediments from central Italy: timing and nature of local and regional Holocene environmental change. *Quaternary Science Reviews* 23, 1699-1722.

Rosignol-Strick, M., 1999. The Holocene climatic optimum and pollen records of sapropel in the eastern Mediterranean, 9000-6000 BP. *Quaternary Science Reviews* 18, 515-530.

Rosignol-Strick, M., Nesteroff, W., Olive, P., Vergnaud-Grazzini, C., 1982. After the deluge: Mediterranean stagnation and sapropel formation. *Nature* 295, 105-110.

Siani, G., Paterne, M., Michel, E., Sulpizio, R., Sbrana, A., Arnold, M., Haddad, G., 2001. Mediterranean sea surface radiocarbon reservoir age changes since the Last Glacial Maximum. *Science* 294, 1917-1920.

Thomson, J., Mercone, D., de Lange, G.J., van Satvoort, P.J.M., 1999. Review of recent advances in the interpretation of eastern Mediterranean sapropel S1 from geochemical evidence. *Marine Geology* 153, 77-89.

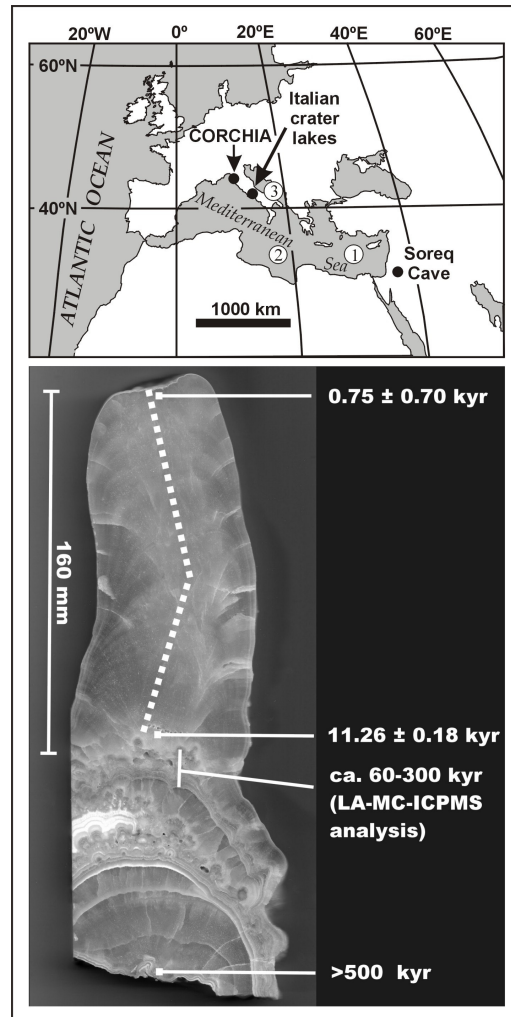


Figure 1 - Upper: The Mediterranean basin showing the location of Antro del Corchia and the main study sites discussed in the text, including the Levantine Basin (1), the Ionian Basin (2) and the Adriatic Sea (3). Lower: Polished section of CC26 stalagmite. Note the popcorn-shaped layers in the lower part of the section indicating slow growth and hiatus. The dashed line indicates the growth axes sampled for stable isotopes analyses. The locations of reconnaissance U-Th analyses (LA-MC-ICPMS: laser ablation multi-collector inductively coupled plasma mass spectrometry) are also shown as reference points.

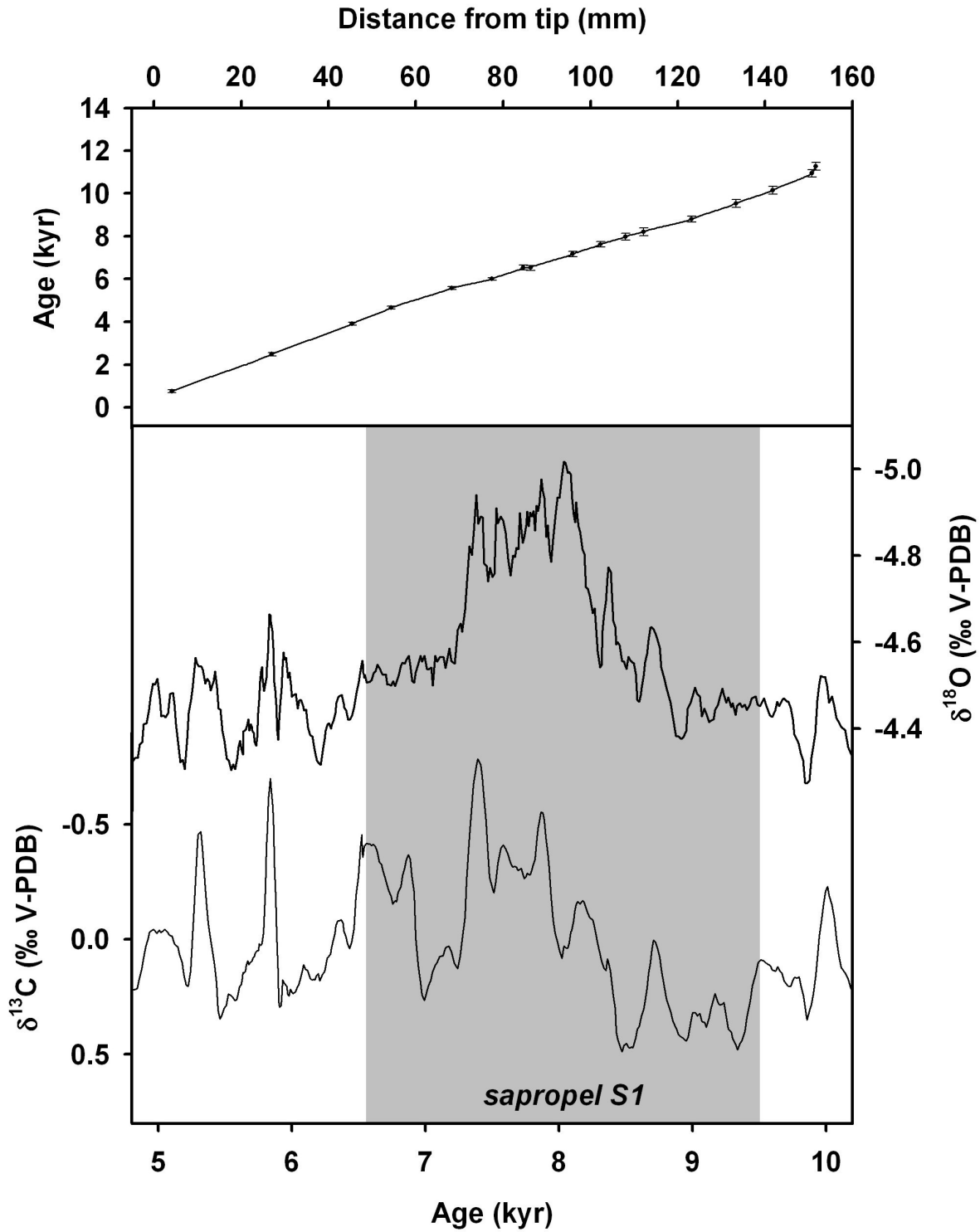


Figure 2 – Upper: depth-age model of CC26. Lower: $\delta^{18}\text{O}$ and $\delta^{13}\text{C}$ time series for the 5-10 kyr period. The shadowed area represents the time of Sapropel S1 deposition according to Emeis et al. (2000). Note that the age of sapropel deposition varies according to different authors.

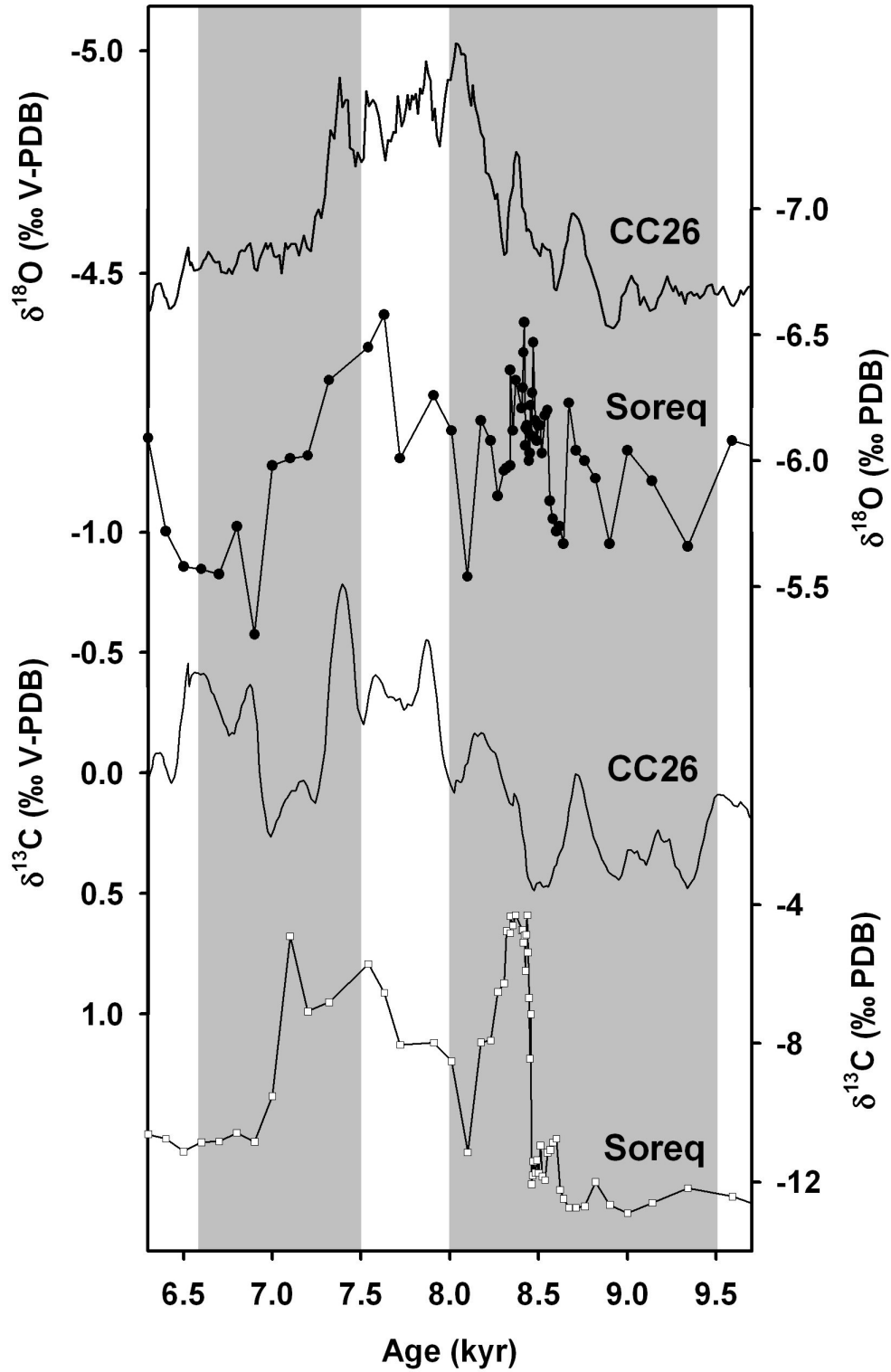


Figure 3 – Comparison between the CC26 isotopic record and the Soreq cave isotopic record during sapropel S1 deposition (the shadowed area as for Fig. 2; the timing of the interruption of S1 is also shown; data from Ariztegui et al., 2000).

Sample	Depth (mm)	U (ppb)	[²³⁰ Th/ ²³⁸ U]	[²³⁴ U/ ²³⁸ U]	[²³² Th/ ²³⁸ U] × 10 ³	Age (kyr)	[²³⁴ U/ ²³⁸ U] _{init}
CC26-4	4.1 (0.3)	6481	0.0046 (4)	0.6639 (13)	0.1068 (15)	0.75 (7)	0.6632 (13)
CC26-5	27.0 (0.3)	4256	0.0151 (4)	0.6643 (13)	0.1982 (15)	2.48 (7)	0.6619 (13)
CC26-3	45.4 (0.3)	4217	0.0235 (4)	0.6652 (14)	0.1719 (70)	3.90 (7)	0.6615 (14)
CC26-6	54.3 (0.3)	4657	0.0278 (4)	0.6647 (18)	0.1116 (20)	4.65 (7)	0.6602 (18)
CC26-7	68.2 (0.3)	4976	0.0333 (4)	0.6690 (15)	0.0531 (7)	5.57 (7)	0.6638 (15)
CC26-2	77.4 (0.3)	5240	0.0359 (4)	0.6714 (13)	0.0502 (25)	6.00 (6)	0.6658 (13)
CC26-8	84.6 (0.3)	4710	0.0390 (6)	0.6719 (16)	0.0357 (6)	6.54 (11)	0.6657 (17)
CC26-9	86.2 (0.3)	5781	0.0391 (7)	0.6745 (15)	0.0246 (11)	6.52 (12)	0.6685 (15)
CC26-10	95.9 (0.3)	4734	0.0430 (8)	0.6767 (19)	0.0305 (18)	7.16 (13)	0.6700 (19)
CC26-11	102.3 (0.3)	4560	0.0452 (7)	0.6718 (15)	0.0136 (6)	7.62 (12)	0.6647 (16)
CC26-12	108.0 (0.3)	5513	0.0475 (9)	0.6744 (14)	0.0419 (28)	7.98 (16)	0.6669 (15)
CC26-13	112.1 (0.3)	5478	0.0487 (10)	0.6737 (18)	0.0245 (14)	8.20 (18)	0.6660 (18)
CC26-14	123.1 (0.3)	4796	0.0522 (8)	0.6755 (14)	0.0166 (17)	8.80 (14)	0.6673 (15)
CC26-15	133.3 (0.3)	4745	0.0565 (10)	0.6775 (18)	0.0125 (13)	9.54 (18)	0.6686 (19)
CC26-16	141.7 (0.3)	5292	0.0597 (10)	0.6750 (20)	0.0292 (15)	10.14 (18)	0.6655 (21)
CC26-1	150.7 (2.0)	4265	0.0639 (9)	0.6729 (20)	0.0224 (17)	10.93 (17)	0.6626 (21)
CC26-17	151.6 (0.3)	6461	0.0659 (10)	0.6744 (17)	0.0199 (11)	11.26 (18)	0.6639 (18)

Table 1. Corrected Th-U ages for stalagmite CC26. The activity ratios have been standardized to the HU-1 secular equilibrium standard, and ages calculated using decay constants of 9.195×10^{-6} (²³⁰Th) and 2.835×10^{-6} (²³⁴U). Depths are from tip, whilst the numbers in brackets are the 95% uncertainties.

Supplementary Material

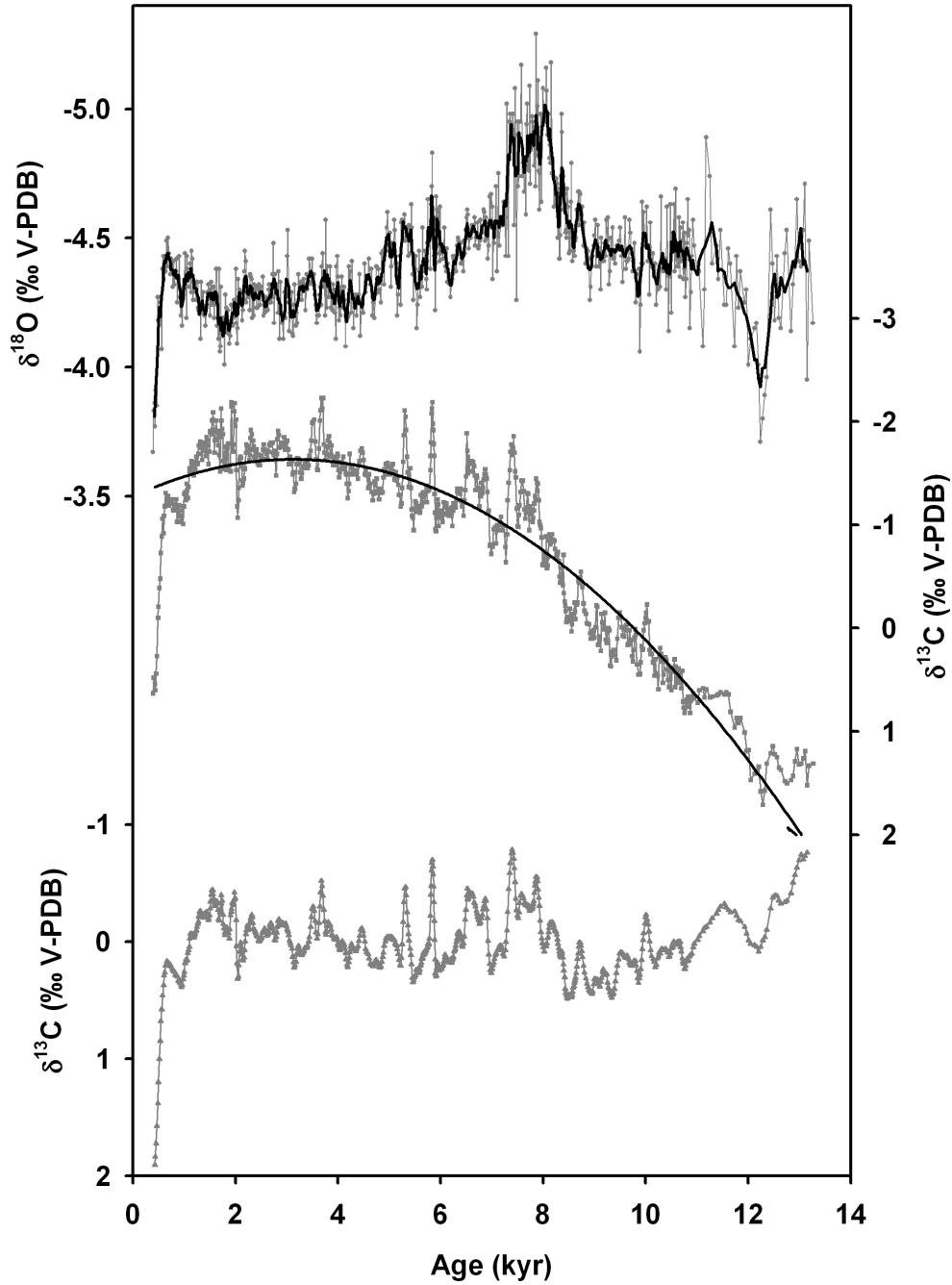


Figure S1 – The complete $\delta^{18}\text{O}$ and $\delta^{13}\text{C}$ time series of CC26 for the upper 160 mm (top two panels). The lower panel contains the detrended $\delta^{13}\text{C}$ time series, where the second order polynomial fit (black line) was subtracted from the raw $\delta^{13}\text{C}$ data.

Methods

Stalagmite CC26 was sectioned longitudinally and micromilled using a lathe housed at the Research School of Earth Sciences, The Australian National University. We used a 200 ± 10 μm sampling interval, which yielded 795 samples. The stable isotope composition of CO_2 gas released by reaction with 105% H_3PO_4 at 70 $^\circ\text{C}$ was measured using an AP2003 mass spectrometer at the SUERC laboratory (Glasgow, UK). Isotopic results are reported using the conventional δ notation in per mille (‰), with reference to the Vienna Pee Dee Belemnite (V-PDB) standard; the $\delta^{18}\text{O}$ of waters cited in the text are quoted with reference to Vienna Standard Mean Ocean Water (V-SMOW). Mean analytical reproducibility ($\pm 1\sigma$) was $\pm 0.06\text{‰}$ and $\pm 0.07\text{‰}$ for carbon and oxygen, respectively.

For U/Th dating, homogenised samples of up to 50 mg were extracted using a 0.7 mm ($n = 15$) and 1 mm drill bits ($n = 2$). Subsamples of ca. 10 mg were dissolved and spiked with a mixed $^{229}\text{Th}/^{233}\text{U}$ tracer before removal of the carbonate matrix using Eichrom TRU-Spec ion-exchange resin. The purified uranium and thorium fraction was introduced in dilute nitric acid to a Nu Instruments MC-ICPMS, where $^{230}\text{Th}/^{238}\text{U}$ and $^{234}\text{U}/^{238}\text{U}$ activity ratios were measured simultaneously using a parallel ion-counting procedure that allows for full internal standardization of ion-counter gain, elemental fractionation and mass bias. Full details of the technique are provided in Hellstrom (2003).